Available online at www.sciencedirect.com
SCIENCE DIRECT®
Journal of Nuclear Materials 324 (2004) 71–75
journal of nuclear materials
www.elsevier.com/locate/jnucmat

Letter to the Editors

Studies on the corrosion behavior of cerium-implanted zirconium

D.Q. Peng *, X.D. Bai, Q.G. Zhou, X.Y. Liu, R.H. Yu, D.L. Zhang

Department of Materials Science and Engineering, Tsinghua University, Beijing 100084, China

Received 19 May 2003; accepted 26 August 2003

Abstract

In order to study the influence of cerium ion implantation on the aqueous corrosion behavior of zirconium, specimens were implanted with cerium ions with a fluence ranging from 1×10^{20} to 1×10^{21} ions/m^2 at about 150 °C, using a MEVVA source at an extracted voltage of 40 kV. The valence and element penetration distribution of the surface layer were analyzed by X-ray photoelectron spectroscopy (XPS) and auger electron spectroscopy (AES) respectively. The potentiodynamic polarization technique was employed to investigate the aqueous corrosion resistance of zirconium in a 1N H_2SO_4 solution. It was found that there was a remarkable improvement in the aqueous corrosion behavior of zirconium implanted with cerium ions compared with that of the as-received zirconium. The corrosion resistance improvement of the cerium-implanted zirconium is probably due to the addition of cerium oxide dispersoid into the zirconium matrix and oxidization protection.

1. Introduction

Because of the low thermal neutron capture cross section, adequate mechanical properties and good corrosion resistance, zirconium and its alloys are often specified for engineering components in the nuclear industry. For example, it can serve as fuel cladding and core structure material. However, with the concept of high burn-up fuel developing, improvements in the performance of zirconium and its alloys are increasingly required. It is well known that ion beam surface processing (IBP) techniques can significantly improve corrosion resistance [1–4]. Ion implantation offers the possibility to introduce a controlled concentration of an element to a thin surface layer. It was first shown by Ashworth et al. that chromium implantation could improve the corrosion resistance of iron [5]. Many works including palladium implanted into titanium [6], phosphorus implanted into iron [7], and molybdenum and tantalum co-implanted into titanium [8] have confirmed that ion implantation can successfully improve corrosion resistance.

Recently, there are many studies about yttrium ion implantation devoted to the investigation of the aqueous corrosion resistance [3,4] and the high temperature oxidation behavior of metals [9–11]. Yttrium and cerium are both rare earth elements, it is expected the implanted cerium had similar effects on the aqueous corrosion resistance comparing to yttrium.

In this paper, cerium implantation was used to study the aqueous corrosion behavior of zirconium. The valences of the cerium ions and absorbed carbon were analyzed by XPS, the depth distribution of elements in the surface layer was determined by Auger electron spectrometry (AES), and the corrosion resistance of the

* Corresponding author. Tel.: +86-10 6277 2856; fax: +86-10 6277 2507.
E-mail addresses: pdq01@mails.tsinghua.edu.cn, baixde@mail.tsinighua.edu.cn (D.Q. Peng).

0022-3115/$ - see front matter © 2003 Elsevier B.V. All rights reserved.
doi:10.1016/j.jnucmat.2003.08.041

implanted zirconium was investigated by the potentiodynamic method using the IM6e potentiostat (Zahner Elektrik Company, Germany). The mechanism of the aqueous corrosion resistance improvement of cerium-implanted zirconium is discussed.

2. Experimental procedure

Zirconium samples were machined to 10 mm × 10 mm from a sheet of zirconium fully annealed after cold rolling. The thickness of the samples was 1.5 mm. The composition of zirconium is Sn: 0.005 wt%, Fe: 0.15 wt%, Ni: 0.007 wt%, Cr: 0.02 wt%, Al: 0.0075 wt%, B: 0.00005 wt%, Cd: 0.00005 wt%, Co: 0.002 wt%, Cu: 0.005 wt%, Hf: 0.01 wt%, Mg: 0.002 wt%, Mn: 0.005 wt%, Mo: 0.005 wt%, Pb: 0.013 wt%, Si: 0.012 wt%, Ti : 0.005 wt%, U: 0.00035 wt%, V: 0.005 wt%, W: 0.01 wt%, Cl: 0.01 wt%, C: 0.027 wt%, N: 0.0065 wt%, H: 0.0025 wt%, O: 0.16 wt%, balanced with zirconium. The zirconium samples were mechanically polished with 200–800 emery paper, subsequently degreased in acetone and ethanol, chemically polished in a solution of 10% HF, 30% HNO_3 and 60% H_2O by volume, rinsed in natural water more than three times and finally rinsed in deionized water.

The samples were loaded onto an aluminum-made sample holder with a diameter of 12 cm. The vacuum level of the target chamber of the MEVVA (metal vapor vacuum arc) implanter was 1.3×10^{-3} Pa. As the implantation has no magnet analysis, the extracted cerium ions were found to consist of 3% Ce^{+}, 83% Ce^{2+} and 14% Ce^{3+}. The fluences were 1×10^{20}, 5×10^{20} and 1×10^{21} ions/m^2; the extracted voltage of cerium implantation was 40 kV. Therefore, the implantation energies were 40, 80 and 120 keV for the Ce^{+}, Ce^{2+}, and Ce^{3+}, respectively. During implantation, the beam current density was 13.3 μA/cm^2, and the maximum temperature of the substrate was 150 °C.

The valence of the cerium ions and carbon on sample surfaces were analyzed by X-ray photoelectron Spectroscopy (XPS). The depth and concentration distributions of elements in the surface layer were determined with PHI-610/SAM Auger electron spectrometer. Potentiodynamic polarization measurements were carried out to investigate the aqueous corrosion resistance of the cerium-implanted zirconium. The potentiodynamic tests were performed in a 1 N H_2SO_4 solution using an IM6e potentiostat at room temperature (25 °C). The tested area was 1 cm^2 and the scan rate was 2 mV/s. All electrochemical potential measurements were taken with respect to a saturated calomel electrode (SCE); measurements were carried out as follows: an anode scan was conducted starting in a cathodic region of approximately −0.4 V with respect to the SCE and scanned into the anodic region of approximately +2.0 V with respect to the SCE.

3. Results and discussion

3.1. The valences of the Ce and Zr in the surface layer

Because of a system error in XPS measurement, the energy position was adjusted by comparing the surface energy of the absorbed C on the surface of the specimen with that of the standard binding energy, 285 eV. In Fig. 1, the surface energy of the absorbed C on the surface of the specimens is 290 eV, which is 5 eV higher than the standard binding energy. The adjusted binding energy of the cerium ions is 882.4 eV (Fig. 2), which coincides with the standard value of CeO_2. Therefore, cerium in the surface exists in the form of CeO_2. The adjusted binding energy of the zirconium $3d_{5/2}$ is 182.4 eV (Fig. 3), which coincides with the standard value of ZrO_2. So zirconium

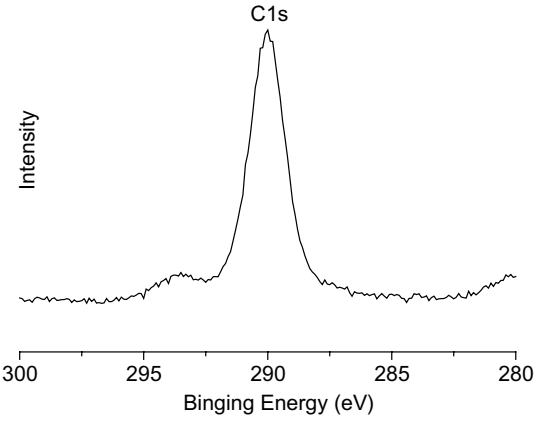

Fig. 1. C 1s XPS spectrum of the implanted surface.

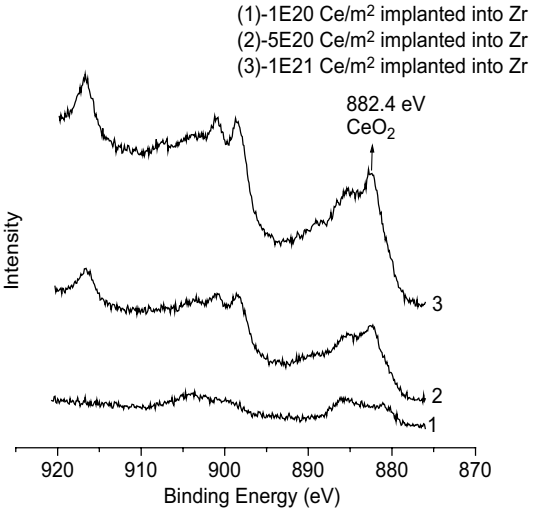

Fig. 2. Ce $3d_{5/2}$ XPS spectrum of the implanted surface.

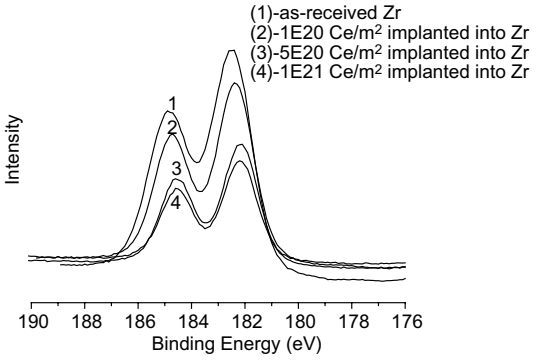

Fig. 3. Zr $3d_{5/2}$ XPS spectrum of the implanted surface.

in the surface exists in the form of ZrO_2. Oxygen comes from the residual gas in the vacuum chamber, since the vacuum level of the target chamber of the MEVVA implanter is not very high. From the AES, it is the fact that the cerium fluence is higher, and that the oxygen element penetration depth is greater.

3.2. Element distribution in the surface layer

AES measurements were taken with a PHI-610/SAM spectrometer to determine the concentration of elements in the oxide film as a function of depth. In the AES measurement, the sputter rate is about 40 nm/min. Fig. 4(1)–(3) respectively show three AES spectra of zirconium implanted with cerium ions to a fluence of 1×10^{20}, 5×10^{20} and 1×10^{21} ions/m^2 respectively. The results show that the peak concentrations of cerium are 10%, 20% and 28% respectively. AES results also show that the depths of the oxide films for the three samples are 24, 152 and 180 nm respectively. It was natural that the depth of the oxide film and the concentration of the elements were mainly determined by the implantation energy and fluence.

3.3. The electrochemical behavior of the cerium-implanted zirconium

Comparing each other, the potentiodynamic polarization curves of the as-received zirconium and the zirconium implanted with cerium ion to a fluence ranging from 1×10^{20} to 1×10^{21} ions/m^2 are summarized in Fig. 5. Fig. 6 plots the passive current density i_p as a function of fluence. The passive current density is defined as follow: the value in the middle of passive region is passive current density, which is the anodic current density at about 0.9 V relative to the SCE.

Comparing the corrosion properties of the cerium-implanted zirconium to that of the as-received zirconium

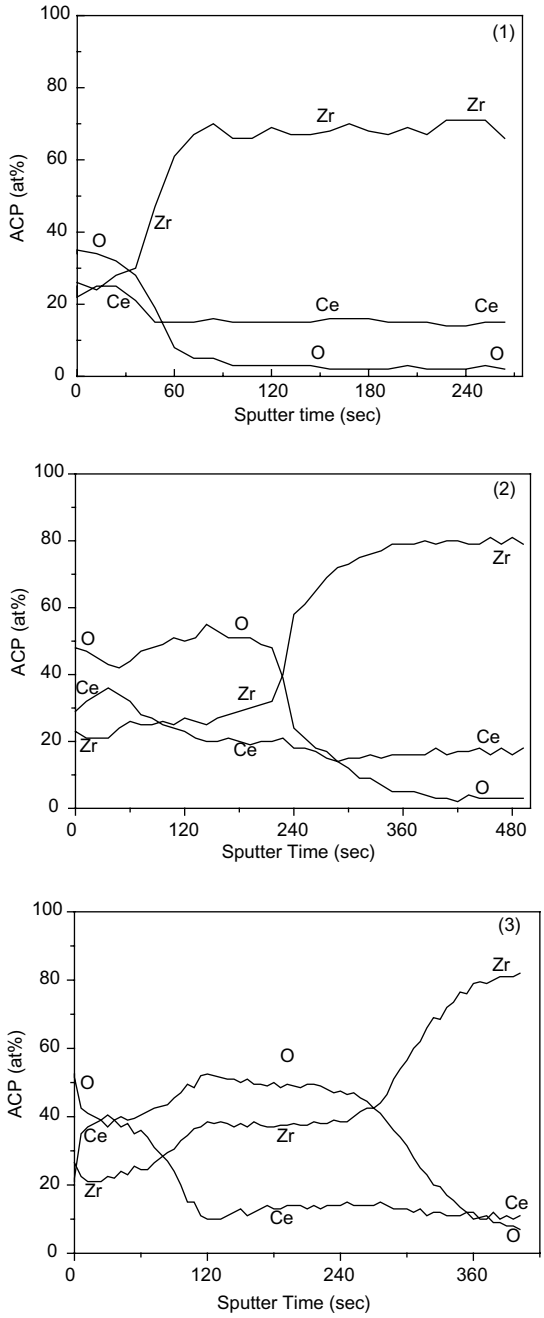

Fig. 4. AES spectra of zirconium implanted with cerium at: (1) 1×10^{20} ions/m^2, (2) 5×10^{20} ions/m^2, and (3) 1×10^{21} ions/m^2.

in Figs. 5 and 6, it is obvious that the passive current density i_p decreases as the implantation fluence increases. It is noted that the aqueous corrosion resistance of zirconium is greatly improved by cerium implantation.

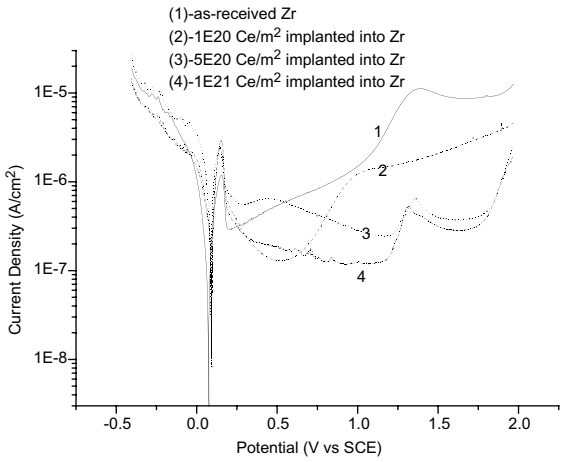

Fig. 5. The potentiodynamic polarization curves of the as-received zirconium and zirconium implanted with cerium ions to a fluence in the range 1×10^{20}–1×10^{21} ions/m^2.

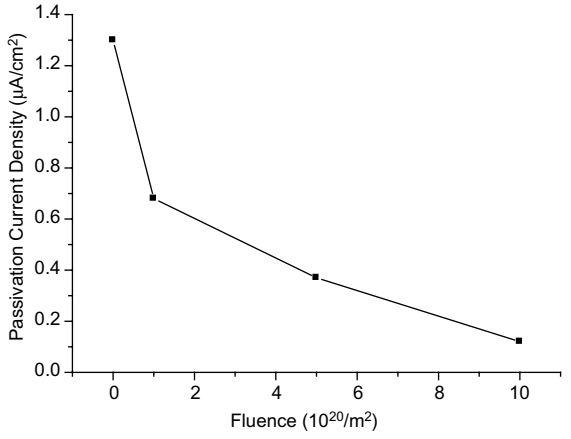

Fig. 6. The relationship between passivation current density, i_p, and Ce fluence.

3.4. The mechanism of the improvement of the aqueous corrosion behavior by cerium ion implantation

It is well known that the formation of the passive film on the surface of zirconium is an oxidation process. According to Pourbaix [12], there is an oxidation reaction that may take place at the zirconium anode:

$$\mathrm{Zr(m)} = \mathrm{Zr^{4+}(aq)} + 4\mathrm{e^-} \quad (1)$$

The cathodic reactions is:

$$\mathrm{H_2O} + \mathrm{H^+} + 2\mathrm{e^-} = \mathrm{H_2(g)} + \mathrm{OH^-} \quad (2)$$

When the anode supplies sufficient Zr^{4+} cations to the solution, $Zr(OH)_4$ immediately became saturated in solution as follows [13]:

$$\mathrm{Zr^{4+}(aq)} + 4\mathrm{OH^-} = \mathrm{Zr(OH)_4(aq)} \quad (3)$$

Based on the facts [12,13], the growth of the film is partially determined by the migration of the zirconium ions.

From the above discussion, the cerium ions existed in the form of CeO_2. The oxide dispersoid addition, CeO_2, acts as a barrier to reduce the migration and dissolution of zirconium [10,14]. When the implanted fluence increases, the concentration of the oxide dispersoid CeO_2 in the surface layer will increases, the migration and dissolution of the zirconium will be more difficult; as a result, the passive current density i_p reduces.

On the other hand, from the AES spectra, it is clear that the depth of the oxide film will increase with implantation fluence. The decrease in the current density could also be attributable to the oxidization protection. When the oxide film grows thick enough to exceed the irradiation range, the irradiation atom could not penetrate the oxide film and the newly formed oxide film layer protects the whole sample from the electrochemical corrosion. But the oxidation process may continue. The thicker the oxide film layer, the lower the passive current density. When the protection of the oxide film exceeds the damage effect of irradiation, the zirconium enters the protection zone. There is another explanation, if the fluence is very high, the amorphization of the matrix metals or alloys would bring out [7,9] which forms a passive film with a very high corrosion resistance and protects the sample, and then the zirconium also goes into its protection zone.

In summary, the greater the implantation fluence, the smaller the passive current density (in the fluence range from 0 to 1×10^{17} ions/cm^2).

4. Conclusions

Cerium ion implantation was carried out on zirconium surface. From the observation of the XPS spectra, the implanted cerium ions and zirconium exist in the forms of CeO_2 and ZrO_2 in the surface layer respectively. A notable improvement was achieved in the aqueous corrosion resistance of zirconium implanted with cerium compared with that of the as-received zirconium. The higher the implantation fluence, the greater the corrosion resistance. The mechanism of the improvement of aqueous corrosion resistance is probably due to the addition of the cerium oxide dispersoid and oxidization protection.

Acknowledgements

Special thanks should be given to the Ministry of Science and Technology of China for research funding

(MSTC No. G 2000067207-1). The authors would like to thank the Analysis Center of Tsinghua University for partial financial support.

References

[1] E. McCafferty, P.M. Natishan, G.K. Hubler, Nucl. Instrum. and Meth. B 56&57 (1991) 639.
[2] Y. Etoh, S. Shimada, K. Kikuchi, J. Nucl. Sci. Tech. 29 (12) (1992) 1173.
[3] J. Xu, X. Bai, Y. Fan, J. Mater. Sci. 35 (2000) 6225.
[4] J. Xu, X. Bai, J. An, Y. Fan, J. Mater. Sci. Lett. 19 (2000) 1633.
[5] V. Ashworth, D. Baxter, W.A. Grant, R.P.M. Procter, T.C. Wellington, Corros. Sci. 16 (1976) 775.
[6] G.K. Huble, E. McCafferty, Corros. Sci. 20 (1980) 103.
[7] X.D. Bai, D.H. Zhu, B.X. Liu, Nucl. Instrum. and Meth. B 103 (1995) 440.
[8] Y. Sugizaki, T. Yasunaga, H. Tomari, Surf. Coat. Technol. 83 (1996) 167.
[9] M.F. Stroosnijder, J.D. Sunderkotter, M.J. Cristobal, H. Jenett, K. Isenbugel, M.A. Baker, Surf. Coat. Technol. 83 (1996) 205.
[10] M.J. Cristobal, P.N. Gibson, M.F. Stroosnijder, Corros. Sci. 38 (1996) 805.
[11] F. He, X. Bai, J. Xu, S. Wang, J. An, Z. Sun, Y. Fan, J. Mater. Sci. Lett. 18 (1999) 715.
[12] M. Pourbaix, Atlas of Electrochemical Equilibria in Aqueous Solutions, N.A.C.E., Houstan, TX, 1974, p. 223.
[13] C.F. Baes Jr., R.E. Mesmer, The Hydrolysis of Cations, Wiley, New York, 1976, p. 147.
[14] K. Przybylski, A.J. Farratt-reed, F.J. Yurek, J. Electrochem. Soc. 135 (1988) 509.